

Single Electron Devices

1 Introduction

We will study tunneling of single electrons in very small tunnel junctions see Figure 1.1. The junctions are typically two metals separated by a thin oxide layer. They are often made by e-beam lithography from aluminum, but also other materials can be used.

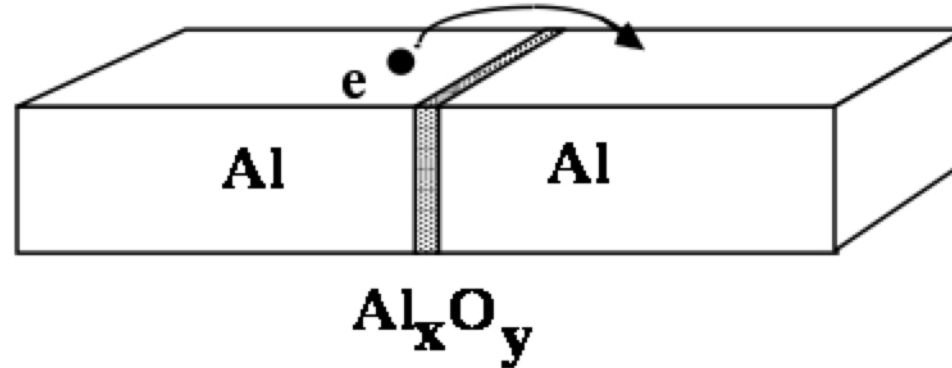


Figure 1.1 A schematic picture of a tunnel junction

Let us start by looking at the tunnel junction as a pure capacitance. If we place a single electron on a tunnel junction it will generate a voltage $V = e/C$. It is obvious that if we make the capacitance very small this voltage will become large. For a typical tunnel junction with an area of $100 \times 100 \text{ nm}^2$ the capacitance will be of the order of 1 fF. Adding an electron to the capacitor results in a voltage of approximately $100 \text{ } \mu\text{V}$.

There is also an electrostatic energy associated with adding a single electron, which is given by $E_C = e^2/2C$. For a junction like the one mentioned above, this energy corresponds to a thermal energy of the order of 1K. To be able to observe single electron tunneling effects we need to satisfy two requirements. First the temperature has to be low compared to the charging energy $k_B T \ll E_C$. This means that we need to cool the sample to low temperatures.

Secondly, to have well defined energy levels, the life time broadening of the energy levels should be small compared to the charging energy itself. This translates into a requirement on the resistance of the junction.

$$\delta E = \frac{\hbar}{2\delta t} \approx \frac{\hbar}{2RC} \ll \frac{e^2}{2C} \Rightarrow R \gg \frac{\hbar}{e^2} = \frac{1}{2\pi} R_K \approx 4.1 \text{ k}\Omega \quad (1.1)$$

The Single Electron devices are best described in terms of charge, where as “ordinary” Josephson devices are best described in terms of phase. Charge and phase are conjugate variables and they obey the quantum mechanical commutation relation $[Q, \varphi] = i\hbar$. This leads to a deep (but not perfect) duality between Single electron devices and Josephson devices. For example the Single Electron Transistor (SET) can be seen as the dual to the SQUID.

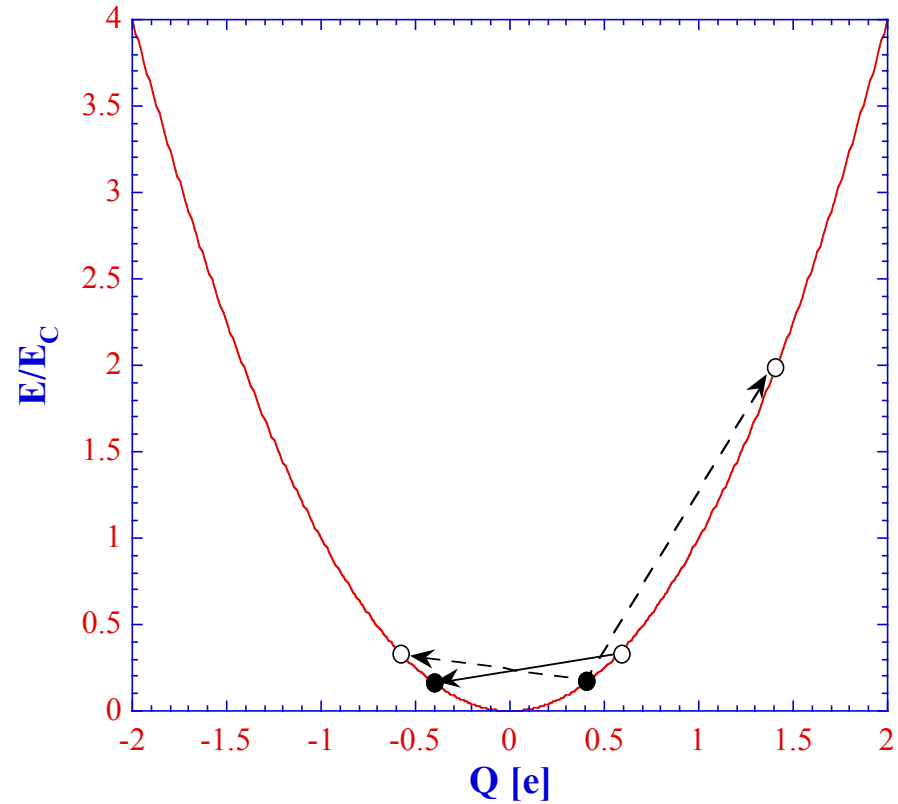


Figure 1.2 Coulomb blockade. For a charge $|Q| < 0.5e$ there are no lower energy states to tunnel to, the tunneling is blocked.

2 The energetics of single electron devices

We start by considering a metallic electrode connected to N independent voltage sources, V_{gi} , via N capacitances, C_i , as shown in Figure 2.1. Let us also assume that there are n excess electrons on the electrode so that the excess charge is $Q = -ne$.

The charge on the common electrode (the island) is just the sum of charges on all the capacitances.

$$Q = \sum_{i=1}^N C_i (V - V_{gi}) = -ne \quad (2.1)$$

Inverting the expression for the charge we get the potential of the electrode as:

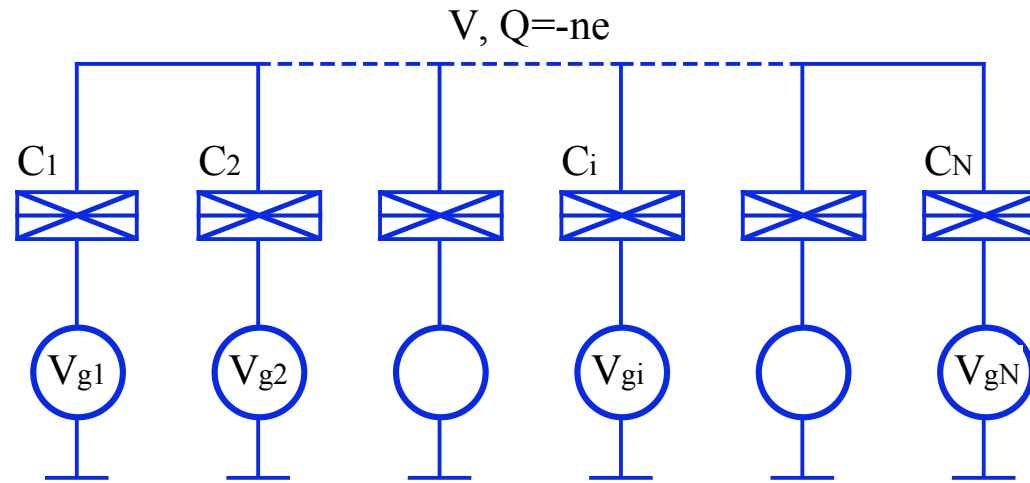


Figure 2.1 A metallic island connected to N independent voltage sources.

$$V = \frac{\sum C_i V_{gi} - ne}{C_\Sigma} \quad (2.2)$$

where C_Σ is the sum of all the capacitances C_i .

The energy of the whole system consists of two parts the electrostatic energy, U , and the work done by the voltage sources, W , as the electrons tunnel onto the island. We get the **electrostatic energy** by simply summing up the energies in the capacitors, *i.e.* the capacitive energy.

$$U = \frac{1}{2} \sum C_i (V_{gi} - V)^2 \quad (2.3)$$

Inserting the expression for the potential V of the island, Eq. (2.2) into Eq. (2.3), we can (after quite a lot of algebra) rewrite this as

$$U = \frac{1}{2C_\Sigma} \sum_{i,j} C_i C_j (V_{gi} - V_{gj})^2 + \frac{n^2 e^2}{2C_\Sigma} \quad (2.4)$$

The **work done by each voltage source** is simply given by the amount of charge that passes through the source, ΔQ_i , times the voltage of the source, V_{gi} . As one electron tunnels onto the island via one of the junctions, lets say junction j , the potential of the island electrode changes by $\Delta V = -e/C_\Sigma$, and the charge is redistributed among the capacitors adding the charge $C_i \Delta V = -eC_i/C_\Sigma$ to each of the capacitors. This means that $\Delta Q_i = +eC_i/C_\Sigma$ has to flow through each voltage source except for source j which also has to supply the extra electron $\Delta Q_j = eC_j/C_\Sigma - e$. The work done by each source is given by $\Delta Q_i V_{gi}$ and thus the total work done by all voltage sources as one electron tunnels in via junction j is:

$$W_j = \sum_i \Delta Q_i V_{gi} = -eV_{gj} + e \sum_i V_{gi} \frac{C_i}{C_\Sigma} = \frac{e}{C_\Sigma} \sum_i C_i (V_{gi} - V_{gj}) \quad (2.5)$$

To get the total work done by the sources we need to add up the terms for all electrons that have tunneled through all the junctions. **Note that for a fixed number of charges on the electrode, this energy is NOT uniquely defined**, since it depends on which junctions the electrons have tunneled in through. Summarizing we can write the total energy for the system as

$$E = U - \sum_j n_j W_j = \frac{1}{2C_\Sigma} \left[\sum_{i,j>i} C_i C_j (V_{gi} - V_{gj})^2 + n^2 e^2 - 2e \sum_j n_j \left[\sum_i C_i (V_{gi} - V_{gj}) \right] \right] \quad (2.6)$$

Now, let us apply this expression to a few important examples.

3 The Single Electron Box (SEB)

The single electron box is the simplest single electron device, see Figure 3.1. We have only two capacitors of which one is a tunnel junction. By applying a negative voltage to the capacitance C_g , we can force electrons to tunnel into the box via the tunnel junction. Using the notations of Figure 2.1, we have the following parameters: $N=2$, $C_1=C_g$, $C_2=C$, $V_{g1}=V_g$, $V_{g2}=0$ and $n_1=0$, $n_2=n$.

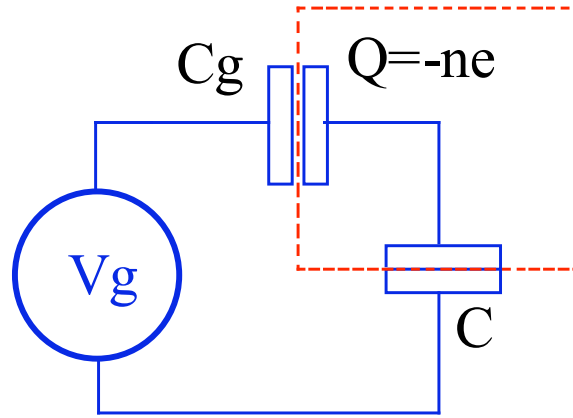


Figure 3.1 A Single Electron Box consists of a junction connected to a voltage source a capacitor. The “box” which holds an integer number of electrons is marked by a red dashed line.

Inserting these notations into eq. (2.6), we get the following expression for the energy of a SEB with n electrons.

$$E(n) = \frac{1}{2C_\Sigma} [CC_g V_g^2 + n^2 e^2 - 2enC_g V_g] = \frac{1}{2C_\Sigma} [C_g^2 V_g^2 + n^2 e^2 - 2enC_g V_g] + \frac{1}{2C_\Sigma} C_g V_g^2 (C - C_g) \quad (3.1)$$

Using the substitution $E_C \equiv e^2 / 2C_\Sigma$ and $n_g \equiv C_g V_g / e$, we get

$$E(n, n_g) = E_C (n - n_g)^2 + E_C \left(\frac{C}{C_g} - 1 \right) n_g^2 \quad (3.2)$$

Note that in this particular case the W_j term is **uniquely defined** since there is only one junction through which the electrons can tunnel into the box. Often the second term in Eq. (3.2) is left out in descriptions of the SEB because it does not depend on the number of electrons in the box, and therefore it does not come in to play when considering tunnel rates, since those only depend on the energy differences between states of different charge.

We can then calculate the gate voltage at which the electron enters the box. This happens when $E(n+1, n_g) < E(n, n_g)$, i.e. when $n_g > 0.5$.

Plotting only the first term of Eq. (3.2) as a function of the external voltage (see Figure 3.2a) we get a set of parabolas one for each n of electrons in the box. Away from the parabola crossings tunneling is not energetically favorable. This is called Coulomb blockade. At the crossings tunneling can occur, which allows the system to stay in its ground state. As the external voltage V_g is increased, the expectation value of the charge increases stepwise as can be seen in Figure 3.2b. This pattern is called the Coulomb staircase.

In some cases the second term in Eq. (3.2) has to be included, *e.g.* if one wants to calculate the capacitance seen by the voltage source. That capacitance can be defined simply as the second derivative of the energy with respect to V_g , and it becomes independent of n .

$$C_S = \frac{\partial^2}{\partial V_g^2} E(n) = \frac{1}{2C_\Sigma} \frac{\partial^2}{\partial V_g^2} [CC_g V_g^2 + n^2 e^2 + 2enC_g V_g] = \frac{CC_g}{C_\Sigma} = \frac{CC_g}{C + C_g} \quad (3.3)$$

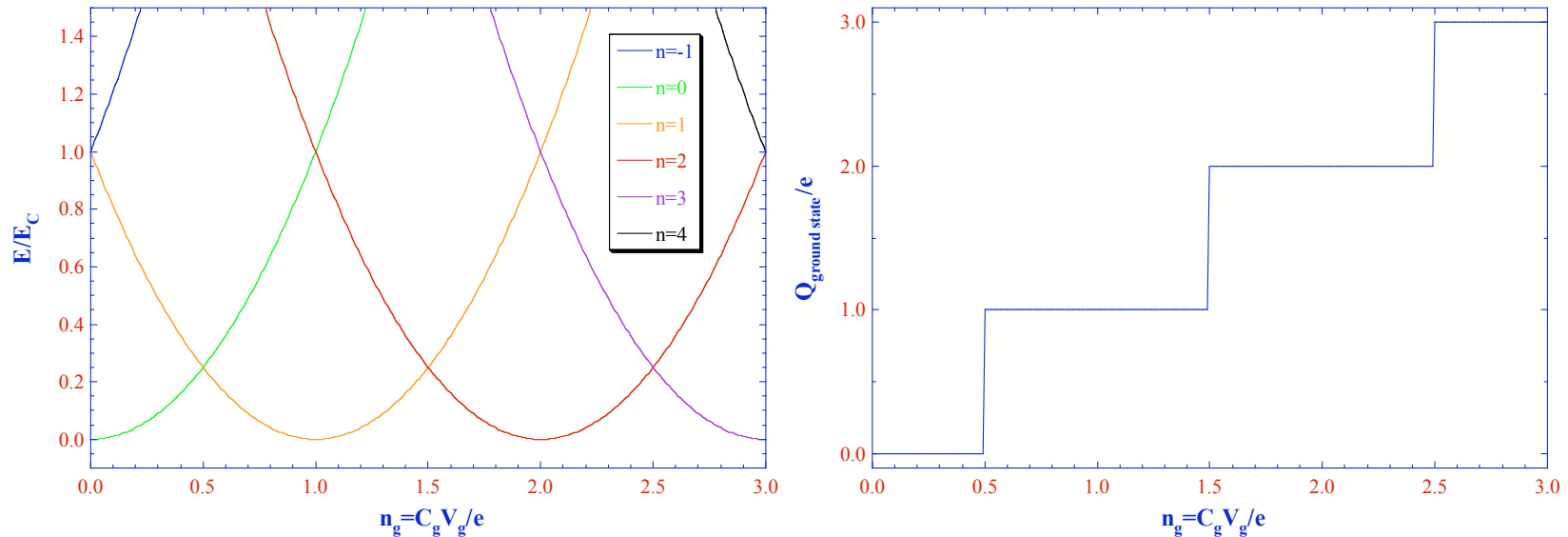


Figure 3.2 a) The energy of the single electron box as a function of external gate voltage. Different parabolas represent different number of electrons in the box. b) The Coulomb staircase, i.e. the expectation value for the charge on the box as a function of external gate voltage.

3.1 Effect of temperature

Figure 3.3 shows a measurement of the charge on a SEB as a function of external voltage, *i.e.* a measurement of the Coulomb staircase. The different curves are for different temperatures. Note that the staircase is smeared by temperature, since tunneling can also occur when the energy difference between two neighboring states are of the order of $k_B T$.

The effect of temperature can be taken into account by assuming a Boltzman distribution between the levels. The average charge becomes

$$\langle n \rangle = \frac{\sum_n n \cdot e^{-E_C(n-ng)^2/k_B T}}{\sum_n e^{-E_C(n-ng)^2/k_B T}} \quad (3.4)$$

If we assume low temperatures, only neighboring states contribute. For example for the transition from 0 to 1 we can simplify this to include only the states $n=0$ and $n=1$.

$$\langle n \rangle = \frac{1}{1 + e^{E_C(1-2ng)/k_B T}} \quad (3.5)$$

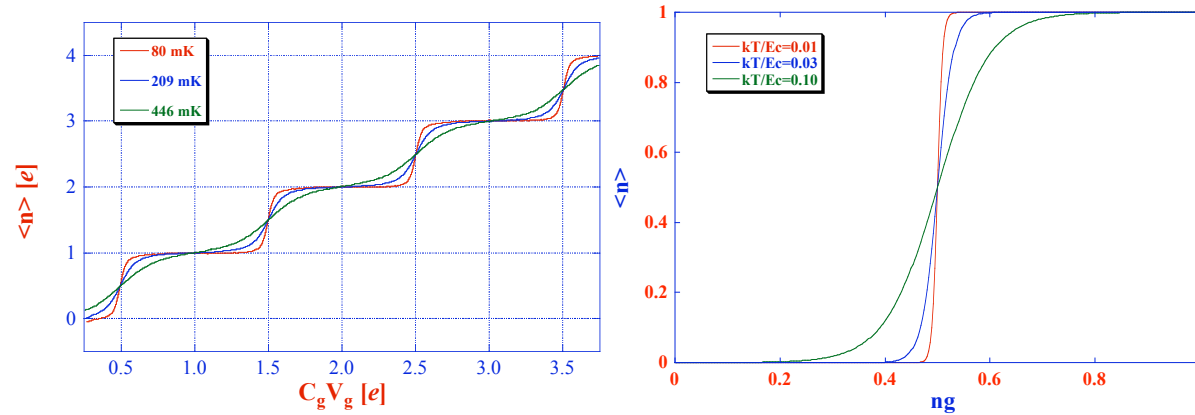


Figure 3.3 a) Measurement of the Coulomb staircase for three different temperatures. b) Calculated smearing of the Coulomb staircase for three different normalized temperatures.

From the smearing of the staircase it is possible to extract the ratio $E_C/k_B T$. Taking such staircases at a well known temperature it is thus possible to extract E_C .

$$\left. \frac{\partial \langle n \rangle}{\partial n_g} \right|_{n_g=1/2} = \frac{E_C}{2k_B T} \quad (3.6)$$

4 The Single Cooper-pair Box (SCB)

The Single Cooper-pair box is very similar to the SEB, with the modification that the electrodes are superconducting, see Figure 4.1. Thus we are interested in the Cooper-pairs rather than the electrons. The energetics for the SCB is the same as for the SEB, but we need to add the Josephson coupling energy E_J . Furthermore, it

is also more convenient to use the $2e$ units such that $n = -\frac{Q}{2e}$, $n_g \equiv \frac{C_g V_g}{2e}$, $E_Q \equiv \frac{4e^2}{2C_\Sigma}$.

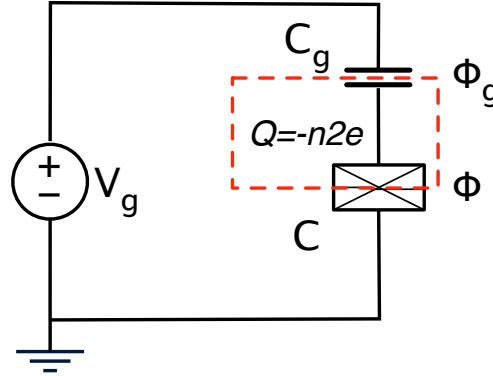


Figure 4.1 A Single Cooper-pair Box (SCB). The cross over the junction indicates that the junction is superconducting and that there is a Josephson coupling energy.

Omitting terms independent of n we can then write the electrostatic energy of the SCB as

$$E(n, n_g) = E_Q (n - n_g)^2 \quad (4.1)$$

This gives the same type of parabolas as in the SEB, except that everything is now in units of $2e$ rather than $1e$. However, we also need to consider the Josephson coupling term, which couples together states which differ in n , *i.e.* it allows for Cooper-pair tunneling on and off the box. This can be seen as avoided level crossings close to half integer n_g -values. We can write down the Hamiltonian as a sum of the two energy terms

$$H = E_Q (n - n_g)^2 - E_J \cos \varphi, \quad (4.2)$$

where φ is the phase difference across the Josephson junction.

To derive the Hamiltonian of the SCB we follow B. Yurke and J.S. Denker, and M.H. Devoret. We start by considering the circuit diagram in . We define the generalized flux as $\Phi(t) = \int_{-\infty}^t V(t') dt'$, where V is either the voltage across the junction or the voltage of the source. We start by writing down the Lagrangian for the system. The kinetic energy T is given by $T = \frac{1}{2} C_g \dot{\Phi}_g^2 + \frac{1}{2} C \dot{\Phi}_J^2$. Using Kirchoffs voltage law we get $\dot{\Phi}_g = V_g - \dot{\Phi}_J$. Subtracting the potential energy we get:

$$L = T - V = \frac{1}{2} C_g (V_g - \dot{\Phi}_J)^2 + \frac{1}{2} C \dot{\Phi}_J^2 + E_J \cos\left(\frac{\Phi_J}{\Phi_0}\right) \quad (4.4)$$

Thus we only have one flux, the conjugate variable to the flux is the charge Q which we get from $Q = \partial L / \partial \dot{\Phi}_J$, we get:

$$Q = -C_g (V_g - \dot{\Phi}_J) + C \dot{\Phi}_J = C_\Sigma \dot{\Phi}_J - C_g V_g$$

$$\dot{\Phi}_J = \frac{Q + C_g V_g}{C_\Sigma}$$

Finally we get the Hamiltonian for the system by doing the Legendre transformation

$$H = Q \dot{\Phi}_J - L = Q \dot{\Phi}_J - \frac{1}{2} C_g (V_g - \dot{\Phi}_J)^2 - \frac{1}{2} C \dot{\Phi}_J^2 - E_J \cos\left(\frac{\Phi}{\Phi_0}\right) =$$

$$Q \frac{Q + C_g V_g}{C_\Sigma} - \frac{1}{2} C_g V_g^2 + C_g V_g \frac{Q + C_g V_g}{C_\Sigma} - \frac{C_g}{2} \left(\frac{Q + C_g V_g}{C_\Sigma}\right)^2 - \frac{C}{2} \left(\frac{Q + C_g V_g}{C_\Sigma}\right)^2 - E_J \cos\left(\frac{\Phi}{\Phi_0}\right) =$$

$$\frac{Q^2 + Q C_g V_g}{C_\Sigma} - \frac{1}{2} C_g V_g^2 + \frac{C_g V_g Q + C_g^2 V_g^2}{C_\Sigma} - \frac{C_\Sigma}{2} \left(\frac{Q + C_g V_g}{C_\Sigma}\right)^2 - E_J \cos\left(\frac{\Phi}{\Phi_0}\right) =$$

$$\frac{Q^2 + 2 C_g V_g Q + C_g^2 V_g^2}{2 C_\Sigma} - \frac{1}{2} C_g V_g^2 - E_J \cos\left(\frac{\Phi}{\Phi_0}\right) =$$

$$\frac{1}{2 C_\Sigma} \left((Q + 2 e n_g)^2 - \frac{C_\Sigma}{C_g} 4 e^2 n_g^2 \right) - E_J \cos\left(\frac{\Phi}{\Phi_0}\right) =$$

The total charge on the box has to be an integer times the Cooper-pair charge, $Q=-n2e$. We also define the Cooper-pair charging energy $E_Q = \frac{e^2}{2C_\Sigma}$, and we arrive at the Hamiltonian:

$$H = E_Q (n - n_g)^2 - E_J \cos\left(\frac{\Phi}{\Phi_0}\right) =$$

again omitting terms independent of n . Writing this in the charge basis $|n\rangle$, *i.e.* the eigenbasis of the charge operator, we get the Hamiltonian

$$H = E_Q \sum_n (n - n_g)^2 |n\rangle\langle n| - \frac{1}{2} E_J \sum_n (|n\rangle\langle n+1| + |n+1\rangle\langle n|) \quad (4.3)$$

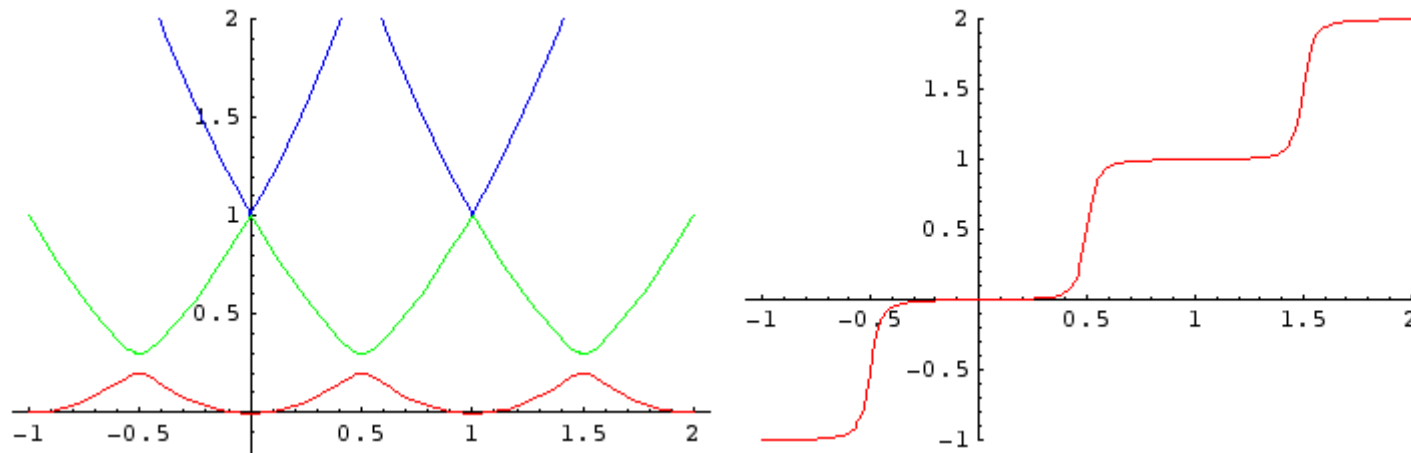


Figure 4.2 a) The energy band diagram of the SCB at zero temperature and $E_J/E_Q=0.1$. b) The Coulomb staircase for the same parameters as in a), note that the staircase is smeared even at zero temperature, this is due to the Josephson coupling energy.

4.1 The two level approximation for small E_J

For small E_J/E_Q ratio the energy bands can be calculated numerically from the n_g dependence of the eigen-energies of the Hamiltonian matrix including a limited number of charge states. The result of such a calculation is shown in Figure 4.2. So called Bloch bands are formed where there are avoided level crossings at half integer values of n_g , *i.e.*, at the points where the charging energy is the same for two neighboring parabolas. These points are referred to as the charge degeneracy points.

Also for the Cooper-pair box we get a Coulomb staircase, but with twice longer and twice higher steps. The staircase is smeared even at zero temperature, which is due to the avoided level crossing. For a comparison between a staircase for a SEB and a SCB see Figure 4.3

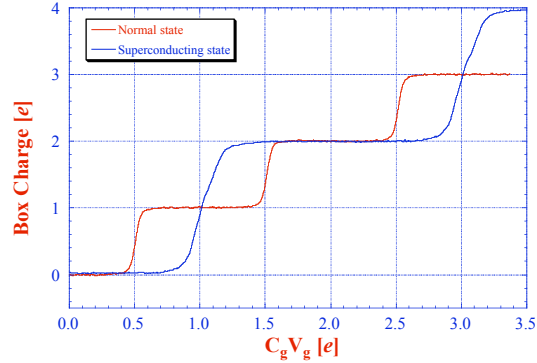


Figure 4.3 A measured Coulomb staircase for a Cooper pair box, blue curve. For comparison a staircase for the same device in the normal state is shown in red in the same graph. The measurements are taken on the same device with (N) and without (S) a strong magnetic field. Note that this experimental graph is presented in le -units.

If we stay close to this degeneracy point and if E_J/E_Q is not too large, we only need to include states corresponding to the two crossing parabolas, lets say $|0\rangle$ and $|1\rangle$. Then the Hamiltonian simplifies drastically and we can solve the problem analytically. This is called the two level approximation or the “qubit approximation” which makes the Hamiltonian equivalent to that of a single spin in a magnetic field. Then we get the Hamiltonian

$$H = E_Q \begin{pmatrix} n_g^2 & 0 \\ 0 & (1-n_g)^2 \end{pmatrix} - \frac{1}{2} E_J \begin{pmatrix} 0 & 1 \\ 1 & 0 \end{pmatrix} = \frac{1}{2} E_Q (2n_g - 1) \begin{pmatrix} 1 & 0 \\ 0 & -1 \end{pmatrix} - \frac{1}{2} E_J \begin{pmatrix} 0 & 1 \\ 1 & 0 \end{pmatrix} + (n_g^2 - n_g + \frac{1}{2}) \quad (4.4)$$

We can then see that this can be written in terms of the Pauli spin matrices.

$$H = \frac{1}{2} E_Q (2n_g - 1) \sigma_z - \frac{1}{2} E_J \sigma_x + E_Q (n_g^2 - n_g + \frac{1}{2}) \mathbb{1} \quad (4.5)$$

4.2 The large E_J limit

For increasing E_J/E_Q we need to add more than two states and the matrix size grows. For large E_J/E_Q this becomes inconvenient. In principle the problem can be solved for arbitrarily large E_J/E_Q if we describe the system in the phase basis. Since Q and φ are conjugate variables we can write $n=Q/2e$ as a derivative of φ . Then the Hamiltonian can be mapped onto the Mathieu equation

$$\left[4E_C \left(-i \frac{\partial}{\partial \varphi} - n_g \right)^2 - E_J \cos \varphi \right] \Psi(\varphi) = E_n \Psi(\varphi) \quad (4.6)$$

which has the following solutions for arbitrary E_J/E_Q .

$$E_m(n_g) = E_C \cdot a_{2[n_g + k(m, n_g)]}(-2E_J/E_Q) \quad (4.7)$$

where m is the energy band index, and $a_\nu(x)$ is Mathieu's characteristic value, with the order ν and the argument $x=-2E_J/E_Q$. The function k is just a sorting function to get the energy bands in the right order. Using for example Mathematica we get a simple way to solve the problem. Bloch bands for three different values of E_J/E_Q are shown in Figure 4.4

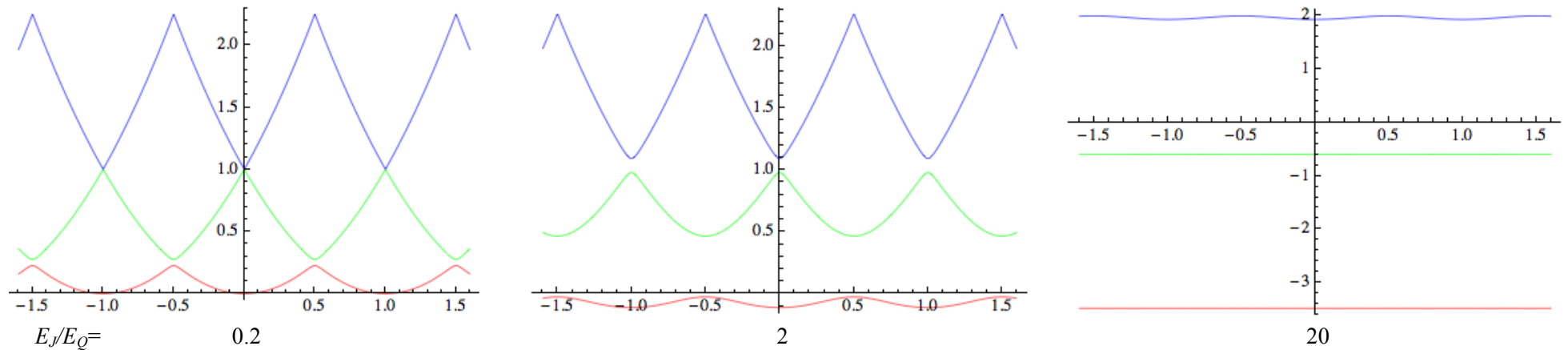


Figure 4.4 Bloch band diagrams for three different values of E_J/E_Q calculated by solving the Mathieu equation. As can be seen the bands get flatter and energy difference between the bands increases with increasing E_J/E_Q .

5 Time correlation, SET and Bloch oscillations

5.1 SET-Oscillations

Let us consider what happens to a single normal junction which is biased by a constant current. The charge on the electrodes will increase linearly with time according to $dQ/dt=I$. As the charge exceeds $e/2$, the tunneling probability increases since ΔE becomes negative and it becomes possible for an electron to tunnel. As one electron tunnels, Q is decreased by the amount e and hence the probability for the next tunneling event decreases. The junction is recharged by the current supply until Q again becomes larger than $e/2$, when the next tunnel event becomes energetically favorable. As a result the tunneling events will occur periodically and not stochastically in time, this is referred to as time-correlated single electron tunneling.

The time interval between tunneling events is determined by charge conservation to be $\Delta t=e/(dQ/dt)=e/I$. Each time an electron tunnels the voltage will drop considerably and then it will increase as the junction is recharged. This means that periodic tunnel events will result in an oscillating voltage as shown in Figure 5.1, with the frequency

$$f_{SET} = I/e \tag{5.1}$$

These voltage oscillations are called Single-Electron-Tunneling Oscillations or simply **SET-Oscillations**. They can be phase locked to external microwaves with the frequency f_{ext} . This gives rise to voltage steps in the dc-I-V curve at currents

$$I = ef_{ext} \tag{5.2}$$

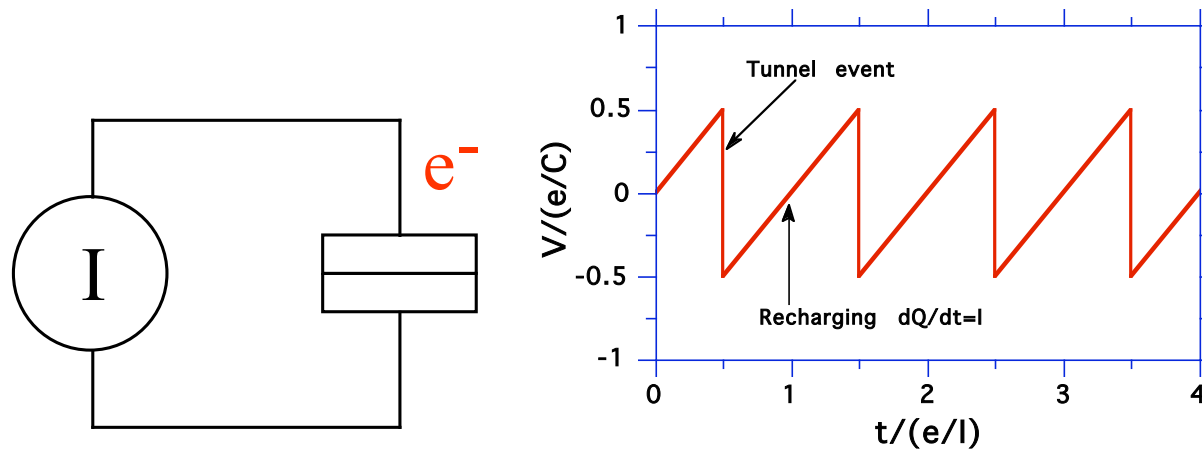


Figure 5.1 a) A current biased small junction. B) The SET-oscillations in a current biased SET junction at low currents ($I \ll e/RC$).

We may interpret the above as follows: each time the microwave field reaches a maximum the tunneling probability is slightly increased and one electron is "helped" to tunnel, during the minimum, the electrons are prevented from tunneling since the tunneling probability is lowered. Harmonics can be understood as helping two or several electrons to tunnel at the maxima, and sub harmonics can be understood as helping one electron to tunnel only every second, third time etc.

Another way to see the phase locking is as a mixing product between the internal and external oscillations resulting in a component at zero frequency i.e. a dc-component in the I-V curve.

Together with the Josephson oscillations and the quantum Hall effect, the SET-oscillations form a "Quantum triangle", see Figure 5.2, in which voltage, current and frequency can be converted to each other by use of the fundamental constants h and e .

The SET-oscillations can be interpreted as the **analog to the ac-Josephson effect**. The time correlated tunneling of single electrons across the barrier in the charging case, corresponds to the time correlated transfer of flux quanta along the barrier in the Josephson case. The single electron tunnel events give rise to an oscillating voltage *i.e.* the SET-oscillations whereas the transfer of single flux quanta give rise to an oscillating current *i.e.* the Josephson oscillations.

The behavior of a microwave irradiated SET junction is very similar to that of a microwave irradiated Josephson junction except for the change of voltage and current. In the same way that the phase locking of the Josephson oscillations gives rise to Shapiro step and is used for maintaining a voltage standard, phase locking to the SET-oscillations could be used for maintaining a current standard.

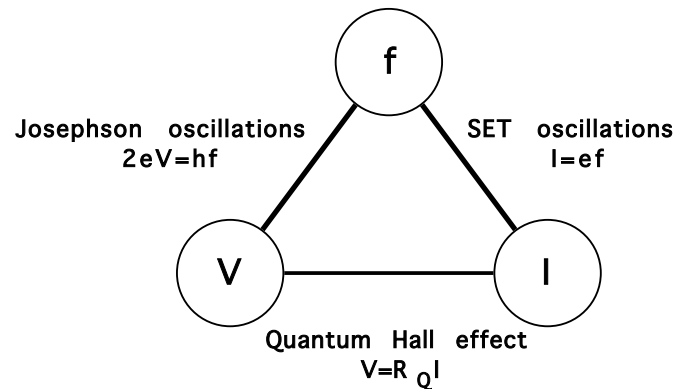


Figure 5.2 The Quantum Triangle.

5.2 Bloch Oscillation

If the Josephson coupling energy E_j is comparable to E_c , energy bands form in the energy diagram. This is very similar to the energy bands which are formed as the periodic potential of the lattice is "switched on" in solid state physics. If an electric field is applied to a solid state crystal the Bloch-electrons may start to oscillate with a frequency directly proportional to the applied electric field and the lattice parameter of the crystal in the field direction.

Similarly, in a small Josephson junction time correlated tunneling of single Cooper pairs may occur, if the quasi particle tunneling is low enough. These correlated tunnel events give rise to voltage oscillations with a frequency $f_{Bloch} = I/2e$.

The small Josephson junction and the solid state crystal can be described with the same type of Hamiltonian. In both cases there is one term parabolic in charge or momentum plus one term periodic in the conjugate variable flux or space coordinate. This analogy gave the name of the voltage oscillations, namely Bloch oscillations.

As we will see in the section 10, it is not easy to current bias a junction and therefore both the SET and the Bloch oscillations are quite difficult to observe.

6 1D arrays of small junctions

To describe a 1-D array of N junctions, we need to specify the capacitance C and resistance R of each junction and the self-capacitance C_0 of each of the interconnecting electrodes. For simplicity the array is assumed to be homogeneous. We neglect capacitive coupling between next nearest neighbors and higher order terms we get the coupling capacitance C between neighboring electrodes only. We describe the system by describing the charge on each electrode (charge nodes) and the voltages of any sources connected to the system (voltage nodes).

For a 1D array with N junctions biased at both ends, we get $N-1$ charge nodes and two voltage nodes. The charges and potentials of the different nodes are related via the following matrix equation:

$$\begin{pmatrix} Q_C \\ Q_V \end{pmatrix} = \begin{pmatrix} C_{CC} & C_{CV} \\ C_{VC} & C_{VV} \end{pmatrix} \begin{pmatrix} \varphi_C \\ \varphi_V \end{pmatrix} = \begin{pmatrix} C_{CC}\varphi_C + C_{CV}\varphi_V \\ C_{VC}\varphi_C + C_{VV}\varphi_V \end{pmatrix} \quad (6.1)$$

For the 1D-array shown in Figure 6.1, the capacitance matrix is given by

$$\begin{pmatrix} C_{CC} & C_{CV} \\ C_{VC} & C_{VV} \end{pmatrix} = \begin{pmatrix} C_0+C & -C & & & & & & & C & 0 \\ -C & & & & & & & & 0 & 0 \\ & C_0+2C & -C & 0 & 0 & & & & 0 & 0 \\ & -C & C_0+2C & -C & 0 & & & & 0 & 0 \\ C_{CC} & C_{CV} & 0 & -C & C_0+2C & -C & & & 0 & 0 \\ C_{VC} & C_{VV} & 0 & 0 & -C & C_0+2C & & & 0 & 0 \\ & & & & & & -C & 0 & 0 & \\ & & & & & & -C & C_0+C & 0 & C \\ C & 0 & 0 & 0 & 0 & 0 & 0 & 0 & C_V & 0 \\ 0 & 0 & 0 & 0 & 0 & 0 & 0 & C & 0 & C_V \end{pmatrix} \quad (6.2)$$

Solving equation (6.1) we get the potentials of the different charge nodes if we know the charges on the charge nodes and the potentials of the voltage nodes.

$$\varphi_C = C_{CC}^{-1}(Q_C - C_{CV}\varphi_V) \quad (6.3)$$

The influence of Josephson coupling is also neglected, *i.e.* $E_J \ll E_C$. The effect of the superconducting energy gap can however be taken into account by assuming a voltage-dependent quasi-particle resistance. The array is assumed to be voltage biased at both ends with a differential voltage V . Using these

approximations some properties of the 1-D arrays can be derived analytically. A schematic picture of the array is shown in Figure 6.1. Voltage nodes can be thought of having very large capacitances to ground and a very large amount of charge.

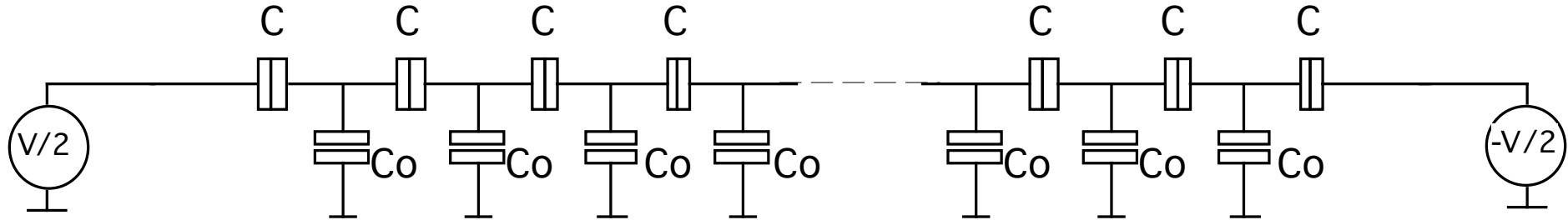


Figure 6.1 Schematic of a homogeneous 1D-array. Each electrode is coupled to its two nearest neighbors by junctions with capacitance C , and to ground by C_0 . The array is typically biased in a symmetric way.

6.1 Charge solitons

A specific property of 1-D arrays is the occurrence of charge "solitons". If a single electron is added to an island inside the array, the surrounding tunnel junction capacitances are charged as well. If the self-capacitances (stray capacitances) of the islands were zero, each junction would be charged an equal amount. With non-zero self-capacitances, the charge has to be shared with the between the junction capacitance and the self-capacitance. Therefore the charge on the junctions will decay with the distance from the initially charged electrode so that the polarization and the charge distribution will be localized in space over a few junctions. The whole charge distribution moves as a single electron is tunneled between islands. The reason for calling this object a charge soliton is that it does not change its form as it moves, provided that it is far from the edges of the array. We can compare with the situation in long Josephson junctions where the magnetic field may tread the tunnel barrier and form flux solitons.

If we place a single electron on the k^{th} electrode of an infinitely long array, a potential φ_k will be generated. This way an effective capacitance is defined, such that $\varphi_k = -e/C_{\text{eff}}$. This effective capacitance is $C_{\text{eff}} = C_0 + 2C_h$, C_h being the capacitance seen from the edge of a half infinite array. It is easy to see that $C_h^{-1} = C^{-1} + (C_0 + C_h)^{-1}$ so that we get

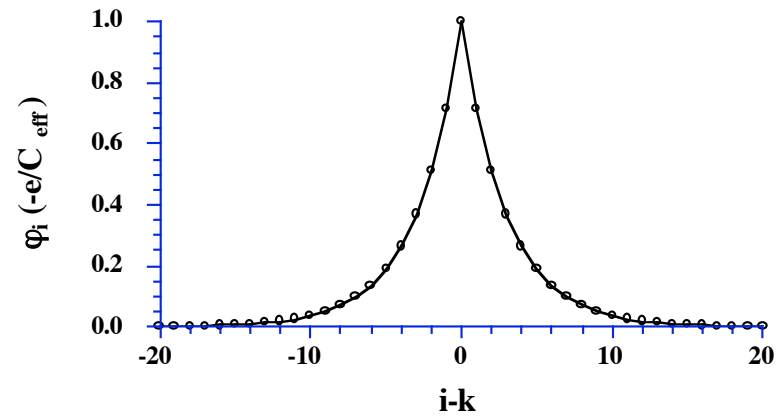


Figure 6.2 The potential distribution created by a single electron placed on an electrode k inside an infinite 1-D array, *i.e.* a charge soliton. The "soliton length" Λ is chosen to be 3. The rings represent the potentials of the electrodes, the solid line is just a guide for the eye.

$$C_h = \sqrt{CC_0 + \frac{C_0^2}{4}} - \frac{C_0}{2} \quad \text{and} \quad C_{eff} = \sqrt{4CC_0 + C_0^2} \quad (6.4)$$

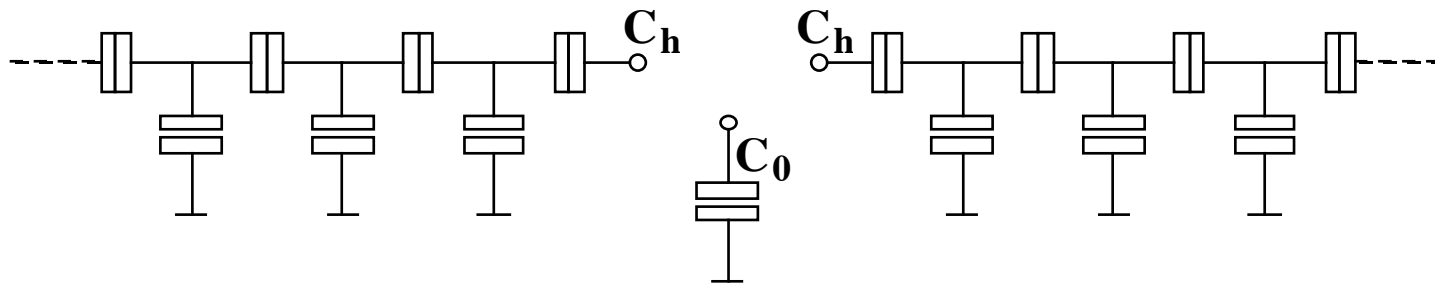


Figure 6.3 The components of the effective capacitance $C_{eff} = C_0 + 2C_h$. C_h is the capacitance of a half infinite array.

For the case of a single electron on the k^{th} electrode there is a potential distribution with a maximum value of $\varphi_k = -e/C_{eff}$. The potential falls off exponentially on both sides as illustrated above. The potential of an arbitrary electrode i as a function of the distance from the charged k^{th} electrode can be calculated. We get

$$\varphi = -\frac{e}{C_{eff}} \left(\frac{C}{C+C_0+C_h} \right)^{|i-k|} = -\frac{e}{C_{eff}} e^{-|i-k|/\Lambda} \quad (6.5)$$

where the fall off constant Λ is the soliton length which is given by

$$\Lambda^{-1} = \ln \left(\frac{C+C_0+C_h}{C} \right) = \ln \left(\frac{C_{eff}+C_0}{C_{eff}-C_0} \right) \approx \sqrt{\frac{C_0}{C}} \quad (6.6)$$

where the approximation is valid when $C > C_0$. It is hard to get a very large number for the soliton length, which is typically less than 5.

6.2 Threshold Voltage

To inject charge into the array you need to overcome the Coulomb blockade by applying a voltage larger than a certain threshold voltage. For a long 1D array biased at one end, the threshold voltage is determined by the voltage at which the first electron enters the first electrode. We can thus treat the rest of the array as a pure capacitor with the capacitance C_h . This problem is in fact very similar to the problem of the SEB, and we have the following situation; $N=2$, $i=1,2$, $j=1$, $C_1=C$, $C_2=C_0+C_h$, $V_{g1}=V$, $V_{g2}=0$, and we can write the energy as:

$$E(n) = \frac{1}{2C_\Sigma} [(C_0+C_h)CV^2 + n^2e^2 - 2en(C_0+C_h)V] \quad (6.7)$$

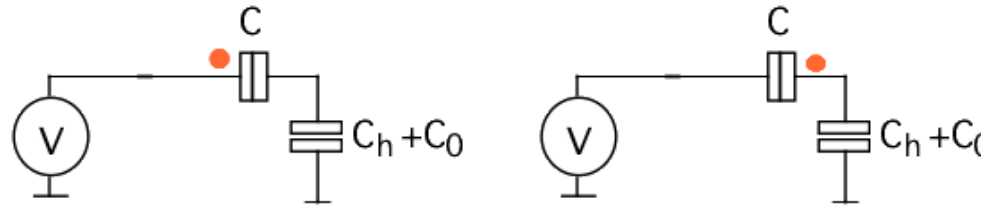


Figure 6.4 Simplified schematic for the first island of a 1D-array. The problem can be mapped onto the SEB. The threshold is the voltage at which the energy of having one electron on the island and the energy of having no electron on the island are equal.

To calculate the threshold voltage for an electron to enter the array we consider the two situations shown in Figure 6.4. The threshold voltage is reached when the states containing $n=0$ and $n=1$ have the same energy, *i.e.* $E(0)=E(1)$. The calculation becomes simpler if we realize that the first term is independent of n and therefore falls out. We can thus easily extract the threshold voltage

$$0 = e^2 - 2e(C_0 + C_h)V$$

$$V_t = \frac{e}{2(C_0 + C_h)}$$
(6.8)

If we consider the threshold for entering a Cooper-pair (assuming small E_J) we get a very similar calculation

$$E(0) = E(2)$$

$$0 = 4e^2 - 4e(C_0 + C_h)V$$
(6.9)

$$V_{t,Cp} = \frac{e}{C_0 + C_h}$$

Finally we consider the threshold for breaking up a Cooper pair and entering a single electron

$$E(0) = E(1) + 2\Delta$$

$$0 = e^2 - 2e(C_0 + C_h)V + 4\Delta C_\Sigma$$
(6.10)

$$V_{t,qp} = \frac{e}{2(C_0 + C_h)} \left(1 + \frac{2\Delta}{E_C} \right)$$

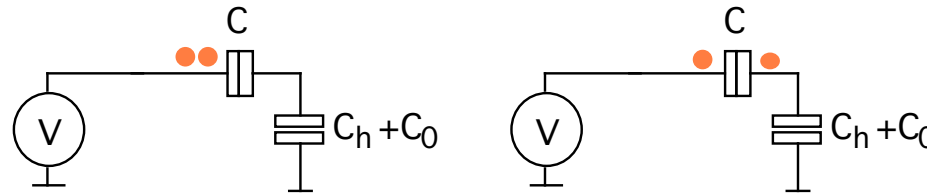


Figure 6.5 Simplified circuit scheme for a biased 1D-array before and after a Cooper-pair has been broken and a single quasiparticle has tunneled into the first island.

7 The Single Electron Transistor (SET)

The Single Electron transistor is a device which is formed by connecting two junctions in series and coupling a third electrode capacitively to the central island. The SET is the most important single electron device since it can be used as a very sensitive electrometer. Let's now use equation (2.6) to look at the energetics of the SET.

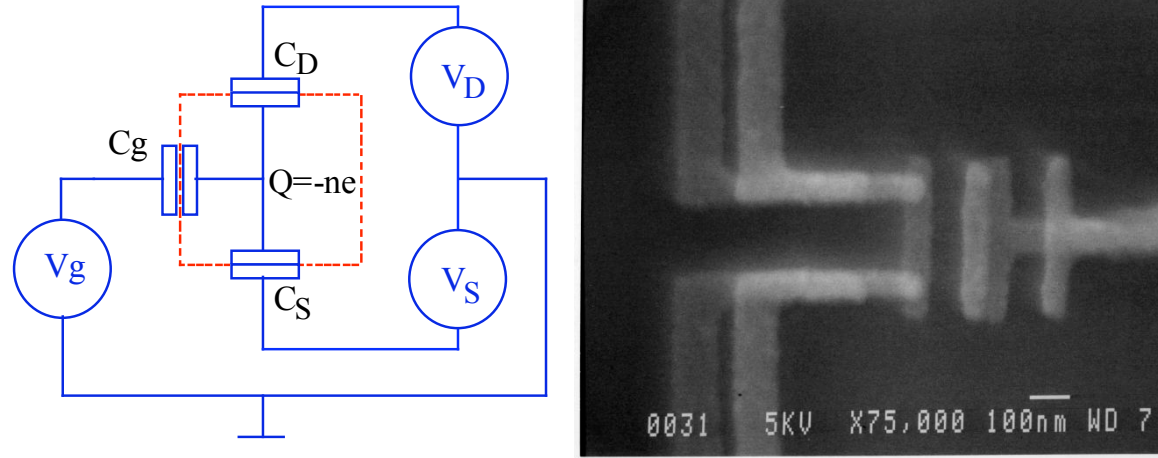


Figure 7.1a) A circuit diagram of the symmetrically biased SET. b) A scanning electron micrograph of an SET.

For the Single Electron transistor we have three terminals: two junctions and the gate capacitance. To simplify thing we apply a symmetric bias, $V_D = -V_S = V/2$. Thus we have the following parameters: $N=3, V_1 = -V/2, V_2 = V/2, V_3 = V_g, C_\Sigma = C_S + C_D + C_g$,

$$E = \frac{1}{2C_\Sigma} \left[n^2 e^2 + \sum_{i,j>i} C_i C_j (V_{gi} - V_{gj})^2 - 2e \sum_j n_j \left[\sum_i C_i (V_{gi} - V_{gj}) \right] \right] \quad (7.1)$$

After some algebra, we arrive with the following expression where only the first two terms depend on the number of electron that has tunneled onto the island

$$E(n_D, n_S) = E_C (n - n_g)^2 + \frac{eV}{C_\Sigma} \left[n_D \left(C_S + \frac{C_g}{2} \right) - n_S \left(C_D + \frac{C_g}{2} \right) \right] + \frac{1}{2C_\Sigma} \left[C_S C_D V^2 + C_S C_g \left(\frac{V}{2} + V_g \right)^2 + C_D C_g \left(\frac{V}{2} - V_g \right)^2 - e^2 n_g^2 \right] \quad (7.2)$$

where we have used the fact that the number of charges on the middle electrode is of course the number of charges entered through the drain plus the number of charges entered via the source, *i.e.* $n = n_D + n_S$. If we set the source and drain voltage to zero, we can see that we recover the expression for the single electron box, *c.f.* eq 3.2. Assuming that an electron tunnels in via the drain junction, *i.e.* $n_D \Rightarrow n_D + 1$, $n \Rightarrow n + 1$, we get the energy difference

$$\Delta E_{D,in} = E(n_D + 1, n_S) - E(n_D, n_S) = E_C \left[(2n + 1 - 2n_g) + \frac{2V}{e} (C_S + C_g / 2) \right] \quad (7.3)$$

To get any tunneling we need to lower the energy, thus the energy difference has to be negative.

$$\Delta E_{D,in} < 0, \Rightarrow V < -\frac{e}{C_S + C_g / 2} \left(\frac{1}{2} + n - n_g \right) \quad (7.4)$$

Similarly, we can calculate the energy difference for tunneling one electron out through the drain junction

$$\Delta E_{D,out} = E(n_D - 1, n_S) - E(n_D, n_S) = E_C \left[(-2n + 1 + 2n_g) - \frac{2V}{e} (C_S + C_g / 2) \right] \quad (7.5)$$

$$\Delta E_{D,out} < 0, \Rightarrow V > \frac{e}{C_S + C_g / 2} \left(\frac{1}{2} - n + n_g \right)$$

and in/out through the source junction

$$\Delta E_{S,in} = E(n_D, n_S + 1) - E(n_D, n_S) = E_C \left[(2n + 1 - 2n_g) - \frac{2V}{e} (C_D + C_g / 2) \right] \quad (7.6)$$

$$\Delta E_{S,in} < 0, \Rightarrow V > \frac{e}{C_D + C_g / 2} \left(\frac{1}{2} + n - n_g \right)$$

$$\Delta E_{S,out} = E(n_D, n_S - 1) - E(n_D, n_S) = E_C \left[(-2n + 1 + 2n_g) + \frac{2V}{e} (C_S + C_g / 2) \right] \quad (7.7)$$

$$\Delta E_{S,out} < 0, \Rightarrow V < -\frac{e}{C_S + C_g / 2} \left(\frac{1}{2} - n + n_g \right)$$

As an example, for $n=0$ we get the following thresholds

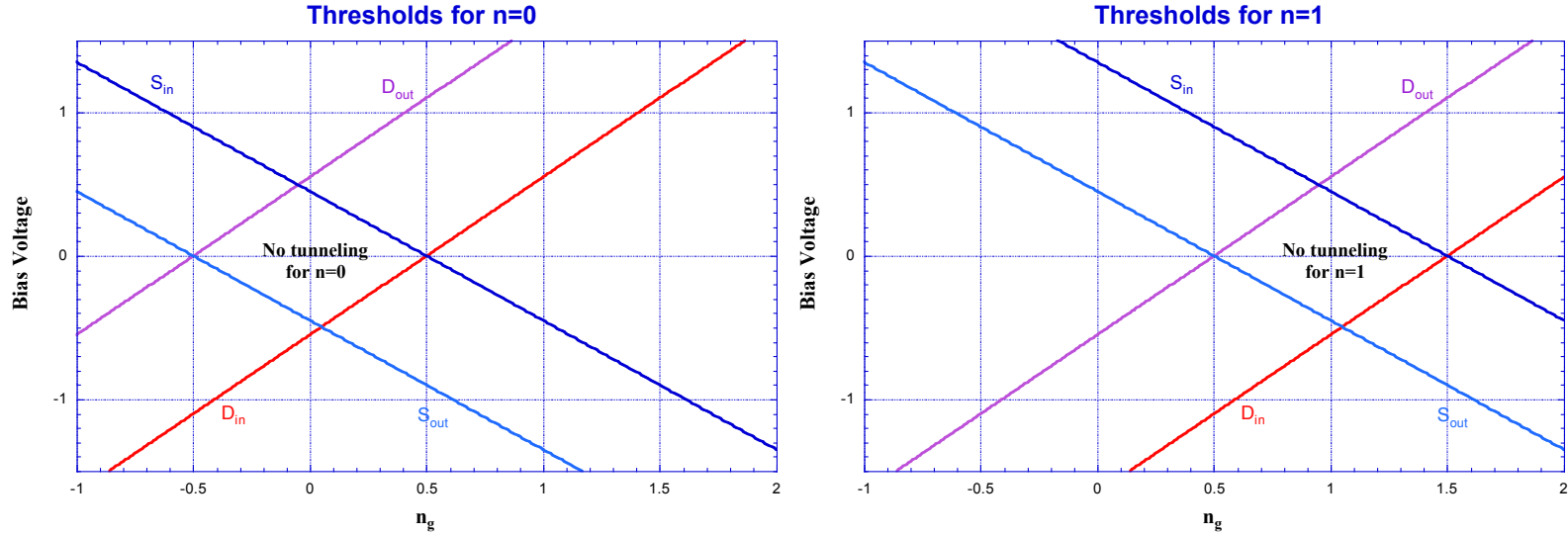


Figure 7.2 Stability diagrams for specific numbers of electrons on the box. a) $n=0$, b) $n=1$.

Note that the threshold for $D_{in}(n=0)$ is identical to the threshold for $D_{out}(n=1)$, and likewise for $S_{in}(n=0)$ and $S_{out}(n=1)$. To get transport through the SET transistor we need to satisfy the condition for tunneling in through one junction and out through the other one. This gives the bias conditions the Coulomb blockade in the SET. For a bias voltage larger than the positive threshold V_{t+} or smaller than the negative threshold V_{t-} we have coulomb blockade.

$$V_{t+} = \min\left(\frac{e}{C_S + \frac{1}{2}C_g}\left(\frac{1}{2} + (n_g - n)\right), \frac{e}{C_D + \frac{1}{2}C_g}\left(\frac{1}{2} - (n_g - n)\right)\right), \quad V_{t-} = \max\left(\frac{e}{C_S + \frac{1}{2}C_g}\left(\frac{1}{2} - (n_g - n)\right), \frac{e}{C_D + \frac{1}{2}C_g}\left(\frac{1}{2} + (n_g - n)\right)\right) \quad (7.8)$$

Since the threshold voltage is periodic in n_g with the period one, it is enough to consider the $n=0$ case. If we in addition define the asymmetry parameter for the SET, $a = \frac{C_D - C_S}{C_\Sigma}$ we can write the thresholds as.

$$V_{t+} = \frac{e}{C_\Sigma} \min\left(\frac{1+2n_g}{1-a}, \frac{1-2n_g}{1+a}\right), \quad V_{t-} = \frac{e}{C_\Sigma} \max\left(\frac{1-2n_g}{1-a}, \frac{1+2n_g}{1+a}\right) \quad (7.9)$$

Considering an asymmetrically biased SET as in Figure 7.3, we get exactly the same expressions as above, if we redefine the asymmetry parameter as

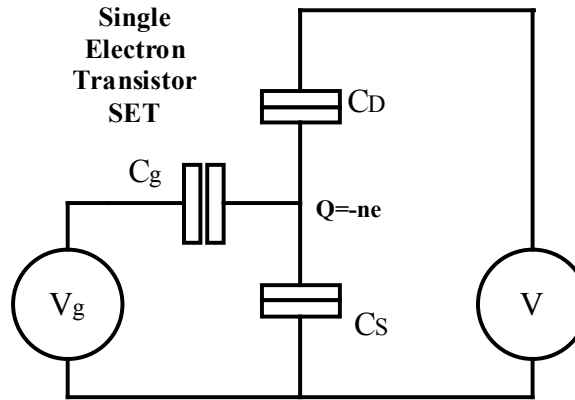
$$a \equiv \frac{C_D - (C_S + C_g)}{C_\Sigma}$$


Figure 7.3 An asymmetrically biased SET

These conditions can be combined into the so called stability diagram for a SET.

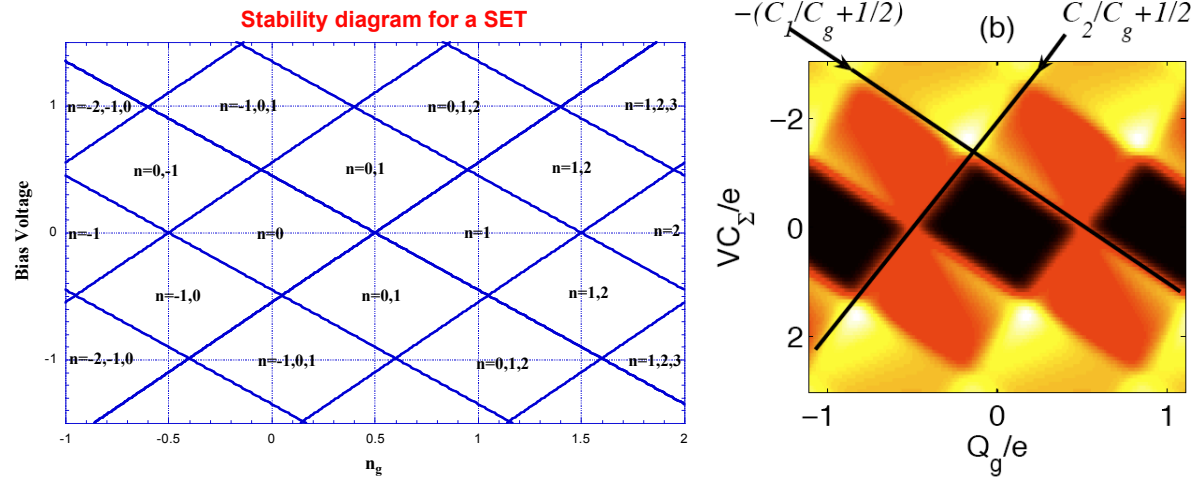


Figure 7.4 a) Calculated diamond plot for a SET. b) Measured diamond plot for a SET, black represents no current, i.e. Coulomb blockade, red and yellow represents the conducting state.

8 Tunneling rates for the SET

We now know in which region of the diamond plot there is current and where there is Coulomb blockade. Now we would like to know how large the current is in the conducting regions. The tunnel rate can be determined by golden rule arguments. From SIS tunnel junctions we are familiar to the tunneling integral, but we now have to take into account the Coulomb blockade and energy conservation, this is done via the delta function. Only tunnel events which can supply the charging energy difference are allowed.

$$\begin{aligned}
 \Gamma_{D,in} &= \frac{1}{e^2 R_D} \int_{-\infty}^{\infty} d\varepsilon_D \int_{-\infty}^{\infty} d\varepsilon_I f(\varepsilon_D) [1 - f(\varepsilon_I)] \delta(\Delta E - (\varepsilon_D - \varepsilon_I)) \\
 &= \frac{1}{e^2 R_D} \int_{-\infty}^{\infty} d\varepsilon_D f(\varepsilon_D) [1 - f(\varepsilon_D - \Delta E)] \\
 &= \frac{1}{e^2 R_D} \int_{-\infty}^{\infty} d\varepsilon_D \frac{1}{1 + e^{\frac{\varepsilon_D}{k_B T}}} \frac{e^{\frac{\varepsilon_D - \Delta E}{k_B T}}}{1 + e^{\frac{\varepsilon_D - \Delta E}{k_B T}}}
 \end{aligned} \tag{8.1}$$

Where we have defined $\Delta E = E(n+1) - E(n)$. This integral can be solved exactly, and the result is the single electron tunneling rate.

$$\begin{aligned}
 &\left[x = e^{\frac{\varepsilon_D}{k_B T}}, \quad dx = \frac{x}{k_B T} d\varepsilon_D, \quad a = e^{\frac{\Delta E}{k_B T}} \right] \\
 \Gamma_{D,in} &= \frac{1}{e^2 R_D} \int_0^{\infty} dx \frac{k_B T}{x} \frac{1}{1+x} \frac{x/a}{1+x/a} = \frac{k_B T}{e^2 R_D} \int_0^{\infty} dx \frac{1}{1+x} \frac{1}{a+x} \\
 &= \frac{k_B T}{e^2 R_D} \frac{1}{1-a} \left[\ln \left| \frac{x+a}{x+1} \right| \right]_0^{\infty} = \frac{k_B T}{e^2 R_D} \frac{\ln|a|}{a-1} \\
 &= \frac{k_B T}{e^2 R_D} \frac{\ln|a|}{a-1} = \frac{1}{e^2 R_D} \frac{\Delta E}{e^{\Delta E/k_B T} - 1}
 \end{aligned} \tag{8.2}$$

$$\Gamma_{D,in} = \frac{1}{e^2 R_D} \frac{\Delta E}{e^{\frac{\Delta E}{k_B T}} - 1} \tag{8.3}$$

This rate is shown in Figure 8.8.1 for a few different temperatures.

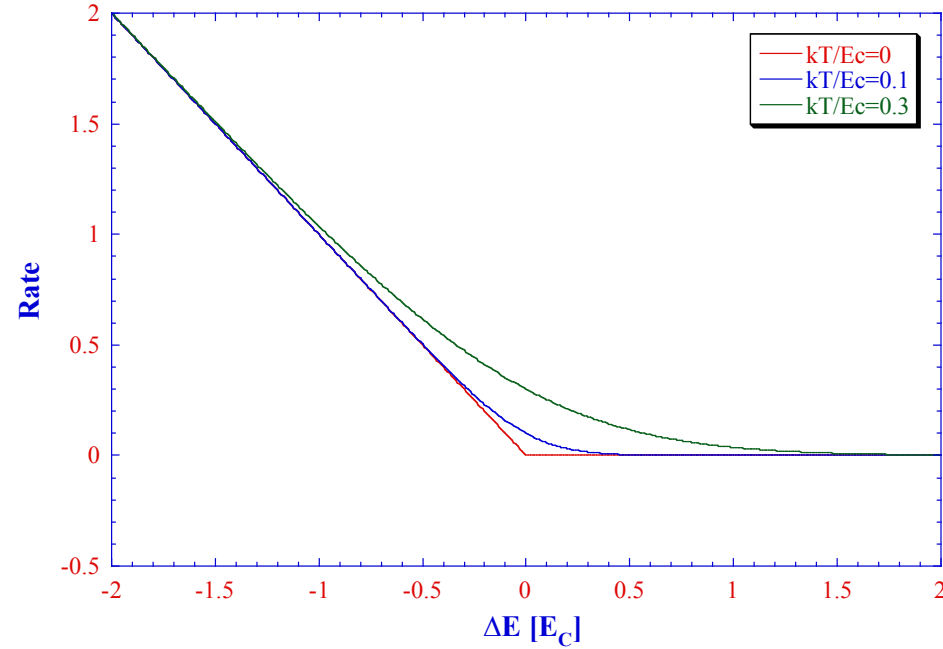


Figure 8.8.1 Tunneling rate versus energy difference ΔE for three different temperatures.

To calculate the current we need the rates in both directions. Furthermore we need the probabilities $P(n,t)$ that there are n electrons on the island.

$$I = I_D = I_S = -e \sum_n (\Gamma_D^+(n) - \Gamma_D^-(n)) P(n,t) \quad (8.4)$$

The probabilities we can get from a master equation

$$\begin{aligned} \dot{P}(n,t) = & -P(n,t) [\Gamma_D^+(n) + \Gamma_D^-(n) + \Gamma_S^+(n) + \Gamma_S^-(n)] \\ & + P(n-1,t) [\Gamma_D^+(n-1) + \Gamma_S^+(n-1)] \\ & + P(n+1,t) [\Gamma_D^-(n+1) + \Gamma_S^-(n+1)] \end{aligned} \quad (8.5)$$

For low currents only low n states are occupied and one can get by with solving this for only 2-3 states, e.g. $n = \{-1, 0, 1\}$. A typical 3D-plot of the IVV_g is shown in Figure 8.2a and a 2D-plot is given in Figure 8.2b. The corresponding IV -curve and IV_g -curves are shown in Figure 8.3.

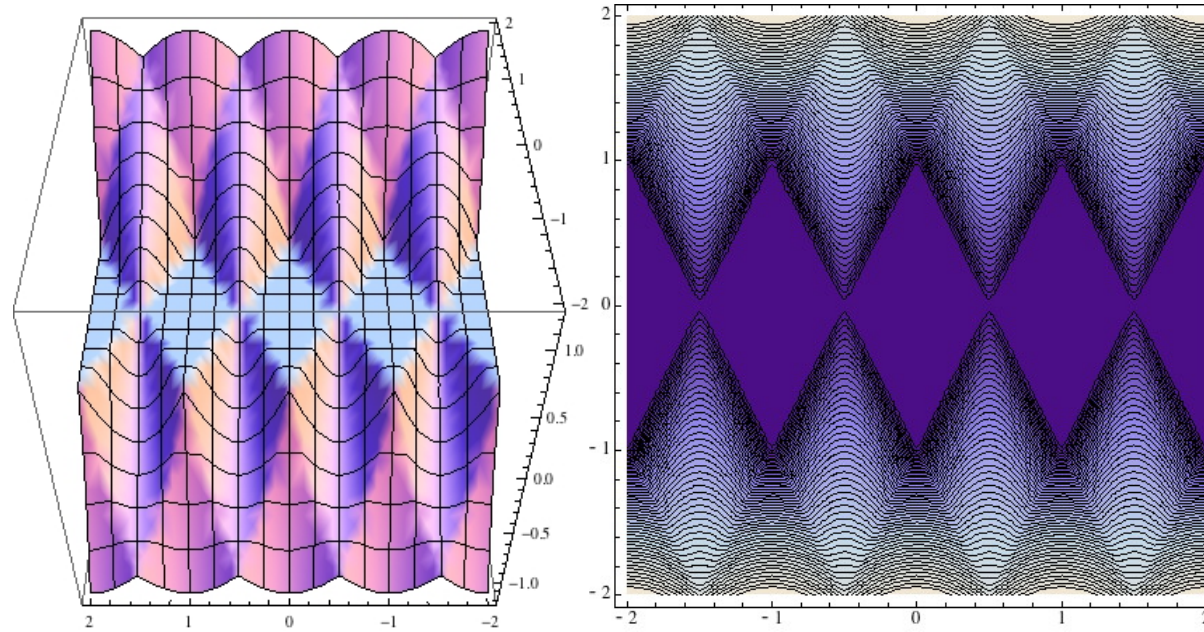


Figure 8.2 a) Current versus bias voltage and gate voltage for a symmetric SET, $k_B T/E_C \approx 0.01$. b) Diamond plot for the same parameters.

Note that in the IV curve when the SET is in the open state (blue curve in Figure 8.3a) the slope is given by $2R_n$. The oscillations in current as a function of gate voltage in Figure 8.3b are called Coulomb blockade oscillations.

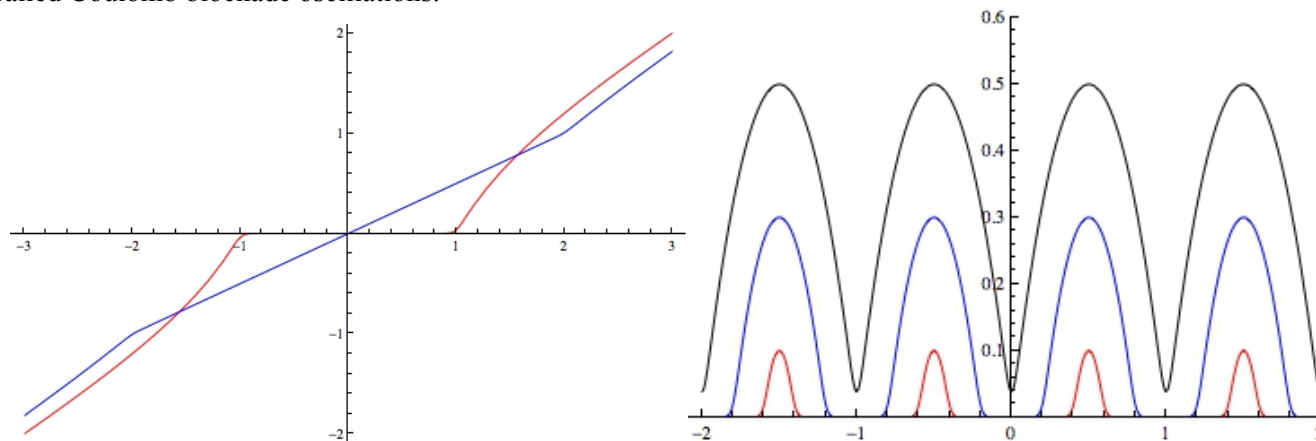


Figure 8.3 a) Current voltage characteristics for two different gate charges. $C_g V_g = 0$ (red) and $C_g V_g = e/2$ (blue). b) Coulomb blockade oscillations, Current as a function of gate charge, for three different bias voltages: $V C_2/e = \{0.2, 0.6, 1.0\}$. $k_B T = 0.01 E_C$ in both plots.

The superconducting SET

There are several modifications if the SET is superconducting. For one there is an energy gap and secondly there are combinations of Cooper-pair tunneling and Single electron tunneling which can occur.

The different processes have different onset conditions which depend on E_C and the superconducting energy gap Δ . The most important ones are Josephson-Quasi-Particle cycle (the JQP cycle) and the double JQP cycle (DJQP).

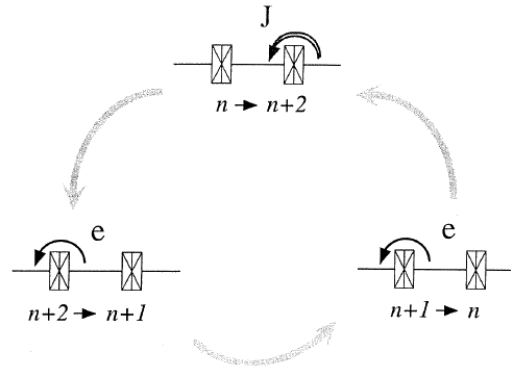


Figure 9.0.1 The Josephson quasi-particle cycle.

In the Table below, you see a list of several different processes. Some of them are resonances giving rise to peaks in the IV-characteristics, where as others are of threshold type which gives rise to steps.

Feature	No. of steps	Cycle Components	Location
SET	2	e, e	T: $4\Delta \leq eV \leq 4\Delta + 2E_C$
supercurrent	2	J, J	P: $eV \approx 0$
JA	2	J, A	P: $\Delta \leq eV$
AA	2	A, A	T: $2\Delta \leq eV$
JQP	3	J, e, e	P: $2\Delta + E_C \leq eV$
AQP	3	A, e, e	T: $3\Delta + E_C \leq eV$
3e	4	J, e, J, e	P: $eV = 2E_C$
3e-A	4	J, e, A, e	P: $\Delta + 2E_C \leq eV$
3e-AA	4	A, e, A, e	T: $2\Delta + 2E_C \leq eV$

=DJQP

Table 6.1: List of current features, the processes which form the cycles, and the bias conditions for which they occur (P = peak, T = threshold).

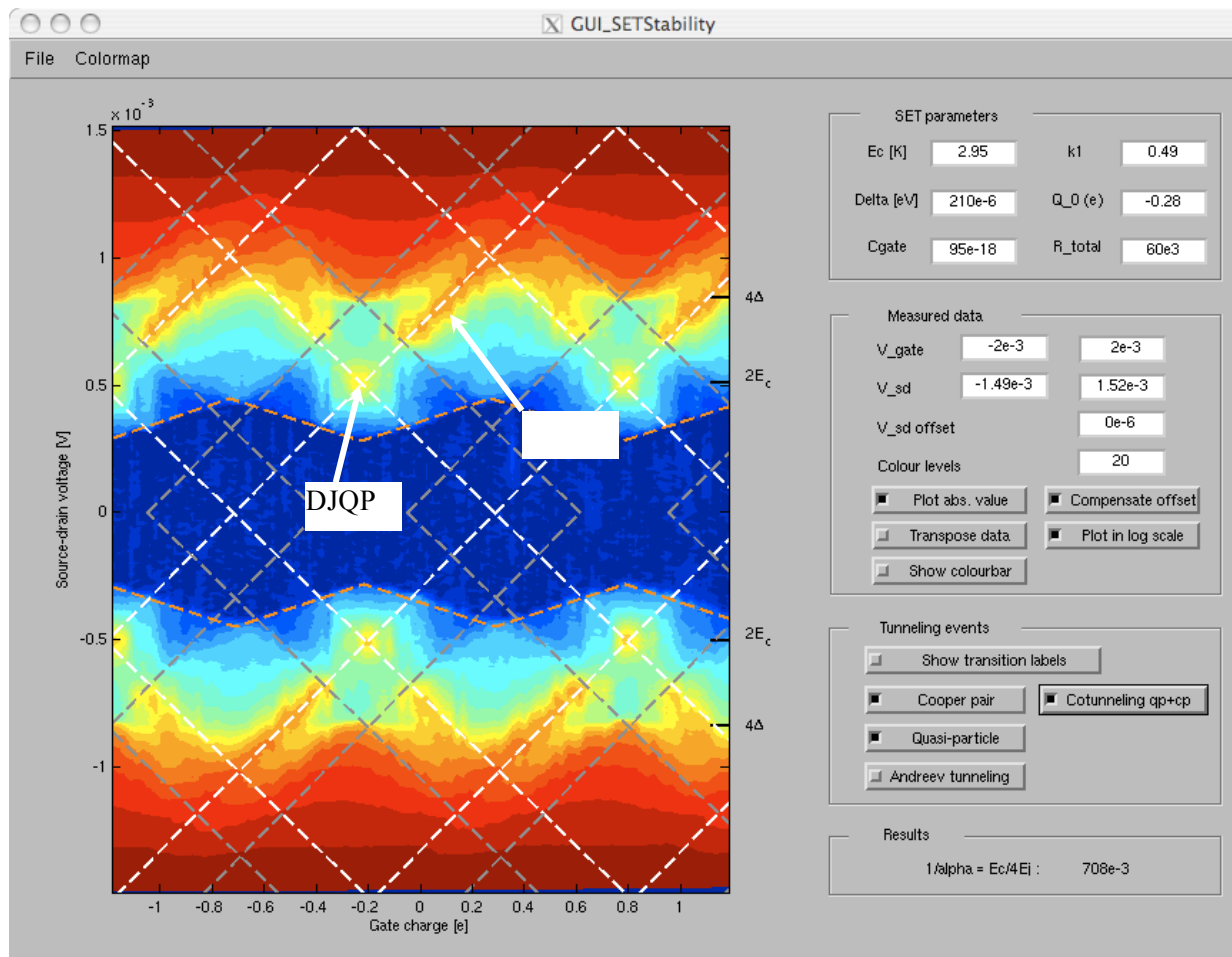


Figure 0.2 Diamond plot for a superconducting SET. The color scale shows the log of the resistance of the SET. The dashed lines correspond to onset of different processes.

9.2 The RF-SET

The frequency limitation of the ordinary SET can be overcome by operating the SET in the RF-mode where the SET is impedance matched to a $50\ \Omega$ coax line using a resonant circuit. An rf signal is launched towards the tank circuits using a directional coupler or a circulator. The reflected signal is amplified by both cold and warm rf-amplifiers and the signal is detected at room temperature. This can be done in two ways either using a “square law detector such as a diode, or by homodyne mixing, i.e. by mixing the reflected signal with the same frequency as you send down.

In both cases the output signal is directly related to the charge on the SET gate.

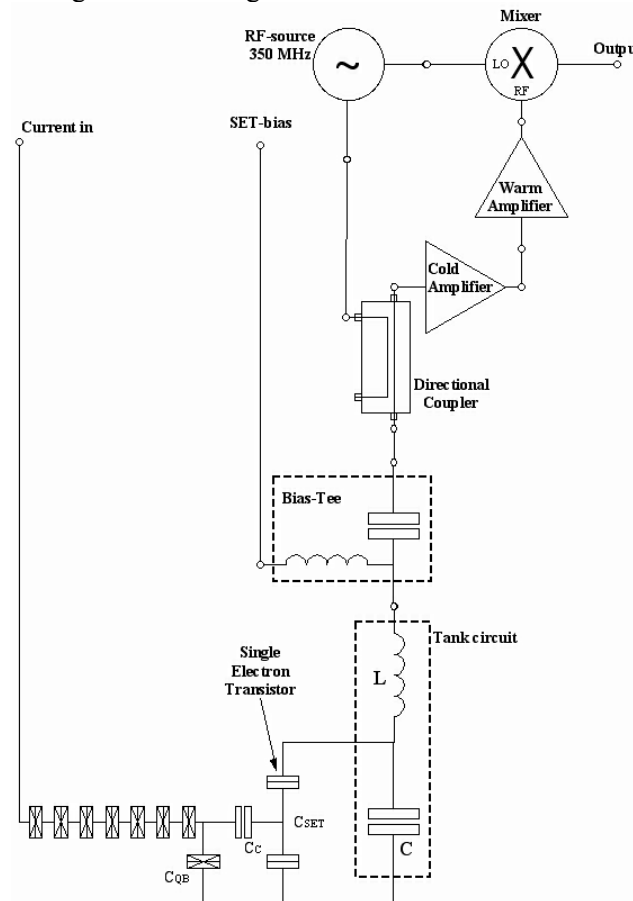


Figure 10.2 Bloch diagram for the RF-SET

We treat the system like an ordinary series resonator with a variable resistor R representing the SET. We make the following definitions: the resonance frequency, $\omega_0 \equiv 1/\sqrt{LC}$, the LC tank impedance, $Z_{LC} \equiv \sqrt{L/C}$, and the quality factors $Q_0 \equiv \frac{Z_{LC}}{Z_0} = \frac{\omega_0 L}{Z_0} = \frac{1}{\omega_0 C Z_0}$, $Q_R \equiv \frac{R}{Z_{LC}} = \frac{R}{\omega_0 L} = \omega_0 C R$ which are referred to as the internal and external Q-values respectively. The impedance seen from the coax line can be expressed as

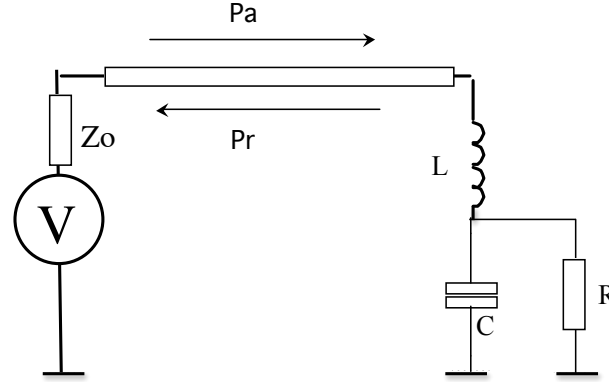


Figure 9.2 Circuit diagram for the reflection measurement of an RF-SET. The wave P_a is launched towards the tank circuit and the wave P_r is reflected.

$$Z_{LRC} = Z_L + Z_{RC} = Z_{LC} \frac{j \frac{\omega}{\omega_0} + Q_R \left(1 - \frac{\omega^2}{\omega_0^2}\right)}{1 + j \frac{\omega}{\omega_0} Q_R} \quad (11.1)$$

which at resonance becomes:

$$Z_{LRC}(\omega_0) = Z_{LC} \frac{j}{1 + jQ_R} = Z_{LC} \frac{1}{Q_R - j} \approx \frac{Z_{LC}}{Q_R} = \frac{Z_{LC}^2}{R} \quad (11.2)$$

where the last approximation is valid if $Q_R \gg 1$, which is normally the case for an RF-SET. Alternatively we can approximate the circuit by a series resonance circuit with an effective resistance

$$Z_{LRC} = Z_L + Z_{RC} = Z_L + Z_C - \frac{Z_C^2}{Z_C + R} \equiv Z_L + Z_C + R_{eff}, \quad R_{eff} = -\frac{Z_C^2}{Z_C + R} \quad (11.3)$$

which at resonance becomes:

$$Z_{LRC}(\omega_0) = Z_L + Z_C + R_{eff} = R_{eff} = \left(\frac{Z_{LC}}{Q_R - j} \right) \approx \frac{Z_{LC}}{Q_R} = \frac{Z_{LC}^2}{R} = \frac{R}{Q_R^2} \quad (11.4)$$

where the last approximation is valid if $Q_R \gg 1$, which is normally the case for an RF-SET. The amount of RF-signal which is reflected at the tank circuit is given by the reflection coefficient Γ .

$$V_r = V_a \Gamma, \quad \Gamma = \frac{R_{eff} - Z_0}{R_{eff} + Z_0} \quad (11.5)$$

where V_a is the available voltage, which in turn is half of the source voltage. We can easily see that perfect matching occurs when

$$R_{eff} \approx \frac{R}{Q_R^2} = Z_0 \Leftrightarrow \frac{Z_{LC}}{Q_R} = Z_0 \Leftrightarrow Q_R = Q_0 \Leftrightarrow Z_{LC} = \sqrt{Z_0 R} \quad (11.6)$$

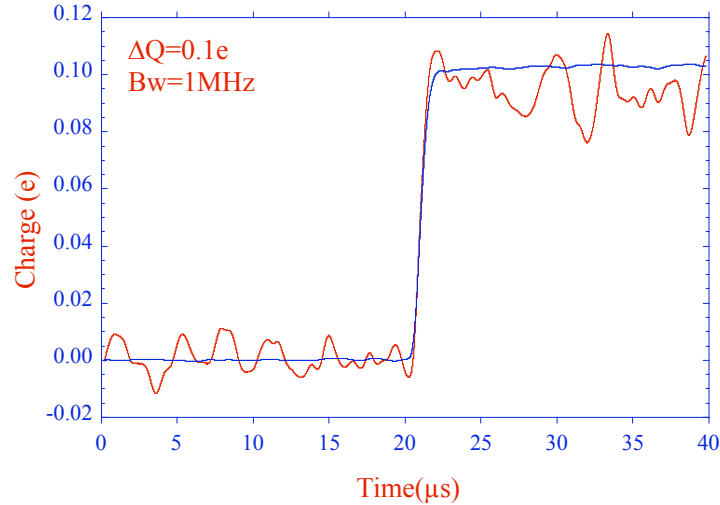


Figure 9.3 A fast measurement of a charge change of $0.1e$, using an RF-SET. the red trace shows a single trace, whereas the blue curve is an average of 512 traces.

The RF-SET can be very fast, speeds up to 100 MHz have been demonstrated. In Figure 9.3 the response to a $0.1e$ step is shown. It can also be very sensitive, charge noise of the order of $1\mu e/\sqrt{\text{Hz}}$ has been demonstrated.

10 The effect of the electromagnetic environment, P(E) theory

If we neglect the effect of the environment of a tunnel junction, the current through a normal tunnel junction is given by

$$I = \frac{1}{eR_N} \int_{-\infty}^{+\infty} [f(E - eV)[1 - f(E)] - [1 - f(E + eV)]f(E)] dE \quad (12.1)$$

Where the Fermi function $f(E)$ is given by

$$f(E) = \frac{1}{1 + e^{E/k_B T}} \quad (12.2)$$

However if the tunnel junction is connected to an external impedance as shown in Figure 10.1, we have to consider the probability for emitting a quanta with the energy $E = eV$ into the environment. The probability density of that process is described by the function $P(E)$. This gives a modified rate

$$\Gamma = \frac{1}{eR_N} \int_{-\infty}^{+\infty} \int_{-\infty}^{+\infty} f(E)[1 - f(E')]P(E + eV - E') dE dE' \quad (12.3)$$

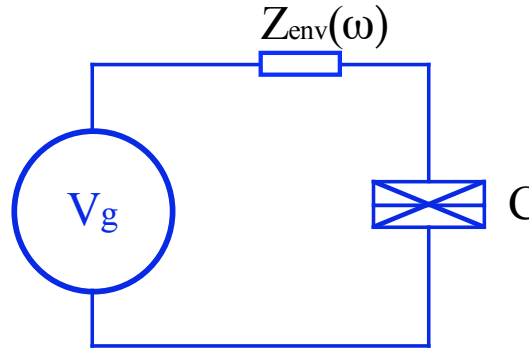


Figure 10.1 Schematic diagram for a junction with environment

Then the current is given by

$$I = \frac{1}{eR_N} \int_{-\infty}^{+\infty} \int_{-\infty}^{+\infty} [f(E)[1 - f(E')]P(E + eV - E') - [1 - f(E)]f(E')P(E' - eV - E)] dE dE' \quad (12.4)$$

which can be simplified to

$$I = \frac{1}{eR_N} \int_{-\infty}^{+\infty} P(eV - E) E \frac{1 - e^{-eV/k_B T}}{1 - e^{-E/k_B T}} dE \quad (12.5)$$

The P(E) function can be expressed as the Fourier transform of another function $P(t)$

$$P(E) = \frac{1}{2\pi\hbar} \int_{-\infty}^{+\infty} e^{i\frac{Et}{\hbar}} e^{J(t)} dt = \frac{1}{\hbar} \int_{-\infty}^{+\infty} e^{i\frac{Et}{\hbar}} \tilde{P}(E) dt = \mathcal{F}^{-1}(\tilde{P}(t)) \quad (12.6)$$

,where $P(t)$ can be written as $\tilde{P}(t) = e^{J(t)}$, and $J(t)$ is the phase-phase correlation function

$$J(t) = \langle [\phi(t) - \phi(0)] \phi(0) \rangle = \langle \phi(t) \phi(0) - \phi(0) \phi(0) \rangle \quad (12.7)$$

The phase ϕ is defined as the integral over the voltage across the junction $\phi(t) \equiv \int_0^t V(t') dt'$

It can be shown that the P(E) function has to fulfill the following normalization and weight condition

$$\int_{-\infty}^{+\infty} P(E) dE = 1, \text{ and } \int_{-\infty}^{+\infty} EP(E) dE = E_C \quad (12.8)$$

For an arbitrary environmental impedance $Z(\omega)$ the correlation function can be written as

$$J(t) = 2 \int_0^{\infty} \frac{d\omega}{\omega} \frac{\text{Re}[Z(\omega)]}{R_Q} \frac{e^{i\omega t} - 1}{1 - e^{-\hbar\omega/k_B T}} \quad (12.9)$$

The relevant impedance, is the external impedance $Z(\omega)$ in parallel with the junction capacitance, C

$$Z(\omega) = \frac{1}{i\omega C + \frac{1}{Z_{env}(\omega)}} \quad (12.10)$$

For a superconducting junction the current is given by: $I_{2e} = \frac{e\pi E_J^2}{\hbar} P_S(E)$, where $P_S(E)$ is the same as $P(E)$ but calculated for a charge of $2e$ rather than e . In other words $\tilde{P}_S(t) = e^{4J(t)}$, where the phase correlation function can be calculated from the environmental impedance. Falci, showed that at $T=0$ the $P(E)$ function obeys the following integral equation, and numerically one can calculate the $P(E)$ function iteratively using it.

$$P(E) = \frac{1}{E} \int_0^\infty \text{Re} \left[Z \left(\frac{E - E'}{\hbar} \right) \right] P(E') dE' \quad (12.11)$$

Let's take an example. For a frequency independent environment of $R=980 \text{ k}\Omega$, and a single tunnel junction with $C=0.4 \text{ fF}$ we get for example the $P(E)$ function shown in Figure 10.1.

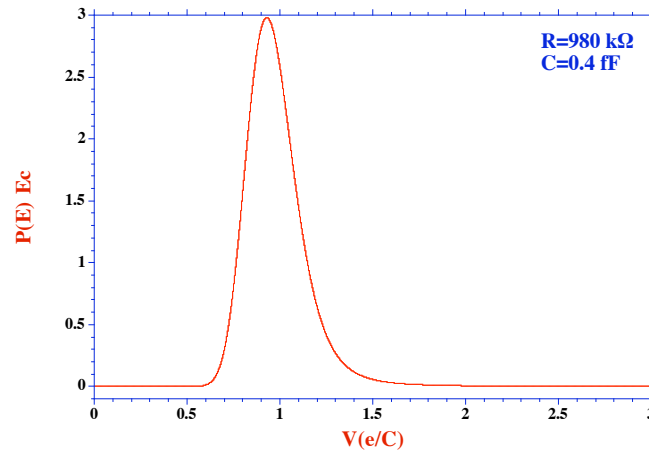


Figure 10.2 In a single junction we would thus get a maximum in the Cooper pair current at $V=e/C$.

11 Cotunneling

There is also a second effect which is neglected in the orthodox theory for single electron tunneling and that is higher order tunnel events, so called cotunneling. This is what happens if two electrons tunnel simultaneously in two different junctions. This takes the system from one state to another state with lower energy, however the intermediate state may have a higher temperature and is thus blocked. This second order tunneling can still happen and is more likely for low tunnel junction resistances.

12 Additional reading

M. Tinkham

in: *Introduction to Superconductivity*, 2nd edition, (ISBN 0-486-43503-2)

Dover Publications, New York, 1996.

Chapter 7, p. 264.

G. Schön

in: *Quantum Transport and Dissipation* (ISBN 3-527-29261-6)

Wiley-VCH Verlag, 1998.

[Chapter 3: Single-Electron Tunneling \(G. Schön\), p. 149-212. \(pdf\)](#)

D. V. Averin and K. K. Likharev

in: *Mesoscopic Phenomena in Solids*, edited by B. L. Altshuler, P. A. Lee and R. A. Webb

North-Holland, Amsterdam, 1991, Vol. 30, p. 173

K.K. Likharev

Reviews

<http://pavel.physics.sunysb.edu/~likharev/nano/PIEE99.pdf>

<http://pavel.physics.sunysb.edu/~likharev/nano/MIGAS03.pdf>

B. Yurke and J.S. Denker, *Quantum network theory*, Phys. Rev. A **29**, 1419 (1984).

M. Devoret, *Quantum fluctuations in electrical circuits*, p351-386, (Les Houches LXIII, 1995) (Amsterdam: Elsevier).